Edge melting and collective edge excitations of the two-dimensional Wigner crystal in a strong magnetic field

R. Côté

Département de Physique et Centre de Recherches en Physique du Solide, Université de Sherbrooke, Sherbrooke, Québec, Canada J1K 2R1

H. A. Fertig

Department of Physics and Astronomy, University of Kentucky, Lexington, Kentucky 40506-0055

The edge electronic structure and collective excitations of a two-dimensional Wigner crystal are studied as a function of the strength of an external static potential that compresses the electrons at the edge of the crystal. It is demonstrated that, as the strength of the external confining potential is increased, the electrons at the edge may melt, giving rise to a phase of the two-dimensional electron gas in which the bulk is essentially crystalline, while the edge is melted. In the generalized random-phase approximation, this melting transition is signaled by the appearance of a collective mode which is gapless even in the presence of pinning centers, and is localized to the edge of the system. The consequences of this melting transition on the transport properties of the system are discussed.

I. INTRODUCTION

As shown by Wigner,[1] a gas of electrons will form a crystal at sufficiently low density and temperature when the energy cost of localizing electrons around lattice sites is outweighed by the decrease in the potential energy due to the formation of the lattice. The Wigner crystal (WC) has effectively been observed some 14 years ago in a two-dimensional electron gas (2DEG) on the surface of liquid helium;[2] however, at the densities attainable in this system, the electron gas is almost classical. To study quantum effects on the electron solid, one must consider systems of higher electron density, such as a 2DEG that is formed at a semiconductor inversion layer or at the interface of a heterostructure. Unfortunately, at least in the heterostructures,[3] the electron density is much higher than the critical density for the observation of the WC and again, the zero-field crystal is not observable. To enhance the possibility of observing the crystallization, a perpendicular magnetic field may be applied to the 2DEG. This forces the electrons to execute circular cyclotron orbits for which the energy is quantized in units proportional to the magnetic-field strength. If the magnetic field is strong enough, all electrons have the minimum quantized kinetic energy, i.e., all are in the lowest Landau level. The large quantized kinetic energy allows the electrons to be localized to a length comparable to their classical cyclotron orbit radius $l = \sqrt{\hbar c / eB}$. Once l becomes small compared to the typical distance between electrons, crystallization will occur. Thus, contrary to the zero-field situation, a Wigner solid will occur for any density if the magnetic field is strong enough. There is currently an active search for observing the WC in $GaAs-Al_x Ga_{1-x} As$ heterojunctions and in metal-oxide-semiconductor field-effect transistor inversion layers.[4] So far, these experiments suggest that the WC has

been observed, although the evidence is not yet conclusive. It seems that a reentrant transition from quantum Hall fluid states [giving rise to the fractional quantum Hall effect (FQHE)] to electron crystal states occurs in sufficiently strong magnetic fields.

Another subject of recent interest is edge effects in the 2DEG in strong magnetic fields.[5] Most work has focused on the integral and fractional quantum Hall effects (IQHE, FQHE), for which theoretical models exist that describe transport on Hall plateaus completely in terms of edge states. In this work as in a previous publication,[6] we focus instead on edge effects in a 2D Wigner crystal in a strong magnetic field. Below, we discuss the behavior of the edge electrons of the crystal when they are subjected to an inhomogeneous external potential, such as the potential at the edge of the positive background of donors, or a potential due to a remote-gate geometry. In Ref. 6, we discussed various edge reconstructions that appear in the presence of a *soft* edge potential that allows the electron density to fall off slowly from its bulk value to zero. In the present paper, we instead discuss phenomena—specifically, edge melting and reconstruction—that occur in the presence of an external potential that tends to *confine* the electrons at the edges. (We note that the case of a confining edge potential which varies on the intermediate length scale of the average interelectron separation has been discussed by one of us.[7])

To study the edge electronic structure of the WC, we use a supercell technique which restores periodicity to the system, reducing the more difficult problem of a finite-size crystal to one that may be handled numerically. The ground state of the crystal is calculated in the Hartree-Fock approximation (HFA) for different values of the confining potential. Once this ground state is known, it is possible to calculate the excitation spectrum

of the crystal, using the generalized random-phase approximation (GRPA), and to discuss its transport properties.

With the above approximations, we show that when the strength of the confinement potential is increased, the edge electronic structure undergoes a reconstruction, followed by a melting transition. In the case where there is reconstruction, there is a noticeable change in the response function that should be observable experimentally. More interesting, however, is the edge melting that occurs at sufficiently strong confining potential. As we show below, this melting transition is signaled by the appearance of a gapless mode in the excitation spectrum that is present even when disorder pins the crystal in the bulk. Interestingly, the excitation spectrum in this case bears a strong resemblance to that of the edge states in the QHE. However, there is an important difference: a calculation of the ground-state current density shows that the melted edge is not chiral. We find local currents in both directions at any given edge, such that the net current at a melted edge vanishes identically, in contrast to the situation in the QHE. The appearance of a gapless mode suggests that the system becomes *metallic* in the melted edge regime, at least within the mean-field (HFA) approximation, even though the WC state is believed to be insulating when edge effects are not important. Our calculations bear out such an interpretation, in that the chemical potential falls in a large gap in the density of states for the unmelted case, whereas at the melting transition, this gap closes up.

However, it is important to recognize that when one goes beyond mean-field theory, the physical situation is likely to be strongly influenced by quantum fluctuations. Below, it will be seen that the melted edge is a quasi-one-dimensional system, so that edge electrons in the melted state may be thought of as a realization of a Luttinger liquid. It has been shown recently[8] that impurities can pin a Luttinger liquid, even though such a system does not generically have long-range translational order. Even in the absence of impurities, the periodic potential seen by the edge electrons due to the bulk (crystallized) electrons can in principle pin them; this was shown explicitly for slowly varying confinement potentials,[7] but may apply in a more complicated way in the present model.[9] Indeed, this system represents a realization of the Luttinger liquid in a periodic potential, for which a complicated set of transitions between pinned and conducting phases has been shown to exist.[9] The phase diagram of this system could, in principle, be mapped out by careful examination of the conductivity of a melted edge as a function of confinement potential and magnetic field.

This paper is organized as follows. In Sec. II below, we introduce the supercell technique that allows us to take into account the finite size of the Wigner crystal. We also introduce there our model Hamiltonian, including the confining potential as well as the pinning potential that simulates the effect of bulk disorder. In Sec. III, we briefly discuss the formalism and numerical method that we use to calculate the ground-state density and current, in the HFA, as a function of the confining potential. Section IV is concerned with the calculation of the density-

density response function as well as collective excitations of the crystal in the GRPA. Finally, our numerical results are presented and discussed in Sec. V. A short account of this work has appeared previously.[10]

II. MODEL AND HAMILTONIAN

The system that we consider consists of a strip of electrons which is infinite along $\hat{x}$ and has a finite width W along $\hat{y}$. Within the strip, the electrons form a triangular lattice with nearest-neighbor separation a_0. A neutralizing positive background of width W is assumed to lie at a distance d below the strip of electrons. (In this work, we shall take $d = 0$. We study the effect of nonvanishing d in Ref. 6.) To model different possible electrostatic environments for the 2DEG, we also consider the effect of an additional local confinement potential $V(y)$ (in practice due to a remote-gate geometry). We take the strength of this confining potential as variable, and study its effect on the ground state of the system when a strong external magnetic field is applied perpendicular to the plane of the strip.

To take into account the finite width of the system, we employ a supercell technique. That is, we assume that the system consists of an infinite number of strips with center-to-center separation A. In this way, the system is made periodic in both $\hat{x}$ and $\hat{y}$ directions. This has the important advantage of allowing us to work with the Fourier transform $\langle \rho(\mathbf{G}) \rangle$ of the ground-state density that we define below. To allow more possibilities for edge reconstructions, we take the unit cell of the system as given by an area of surface $\xi a_0 \times A$ and containing N_c electrons. That is, the unit cell has length ξa_0 in the $\hat{x}$ direction. Classically, the positions of the electrons are then given by

$$\mathbf{r}_{i,\alpha} = \mathbf{R}_i + \mathbf{r}_\alpha \ , \tag{1}$$

where $\mathbf{R}_i$ is the position of the unit cell and $\mathbf{r}_\alpha$ the position of the electron α in this unit cell. The positions $\{\mathbf{R}_i\}$ form a rectangular lattice, that can be described by the discrete set of reciprocal-lattice vectors

$$\mathbf{G} = \left[\frac{2\pi n_x}{\xi a_0}, \frac{2\pi n_y}{A} \right] \ , \quad n_x, n_y = 0, \pm 1, \pm 2, \ldots \ . \tag{2}$$

In principle, to recover the result for a single strip, we must let $A \to \infty$. In practice, we use large enough values for A that our qualitative results no longer change as A is increased. We find that for our present purposes, very large values of A are not actually required. The extent to which it is possible to discuss the large A limit within our numerical approach is addressed in Sec. V.

In the strong-magnetic-field limit that we consider, the filling factor of the total system is given by $\nu = N/g$ (N is the total number of electrons in the system and g is the Landau levels degeneracy). This filling factor is related to the filling factor in a strip ν_s by the relation

$$\nu = \nu_s \left[\frac{W}{A} \right] \ . \tag{3}$$

To respect charge neutrality, the density of the positive background must then be given by

$$n_b = \frac{N_c}{\xi a_0 W} , \tag{4}$$

where N_c is the number of electrons in a unit cell.

In the strong-field limit, i.e., $\hbar\omega_c \gg e^2/l$ ($\omega_c = eB/mc$ is the cyclotron frequency and e^2/l characterizes the strength of the Coulomb interaction), we can make the usual approximation of neglecting Landau-level mixing and restricting the Hilbert space to the first Landau level. It is thus convenient to define a new density operator $\rho(\mathbf{q})$ by the relation

$$n(\mathbf{q}) = g e^{-q^2 l^2/4} \rho(\mathbf{q}) , \tag{5}$$

where the Gaussian form factor reflects the wave functions of the electrons in the lowest Landau level. In terms of this operator, the Hartree-Fock approximation (HFA) for the Hamiltonian of the two-dimensional electron gas in the strong-magnetic-field limit takes the simple form[11]

$$H = \left[\frac{g\hbar\omega_c}{2}\right]\rho(0) + g\sum_{\mathbf{G}} \left[U(\mathbf{G}) + \sum_i \phi_i(\mathbf{G}) \right]\rho(\mathbf{G}) , \tag{6}$$

where the potentials ϕ_i are defined below, and the quantities $\langle\rho(\mathbf{G})\rangle$ can be considered as the order parameters of the crystal phase. (In the homogeneous phase, only $\langle\rho(0)\rangle$ is different from zero.) In Eq. (6), U is the self-consistent Hartree-Fock field produced by the electron lattice, and is given by

$$U(\mathbf{G}) = \left[\frac{e^2}{l}\right] \left[\frac{1}{Gl} e^{-G^2 l^2/2}(1-\delta_{\mathbf{G},0}) \right.$$

$$\left. - \sqrt{\pi/2} e^{-G^2 l^2/4} I_0(G^2 l^2/4) \right]\langle\rho(\mathbf{G})\rangle$$

$$= \left[\frac{e^2}{l}\right][H(\mathbf{G})(1-\delta_{\mathbf{G},0})-X(\mathbf{G})]\langle\rho(\mathbf{G})\rangle , \tag{7}$$

where I_0 is the modified Bessel function of the first kind. The factor $(1-\delta_{\mathbf{G},0})$ arises because the diverging part of the HF potential is cancelled by the $\mathbf{G}=0$ part of the interaction with the nonhomogeneous positive background.

Since the confinement, pinning, and background potentials all couple with the electron density through the usual $-e\int d\mathbf{r}\, n(\mathbf{r})\phi_i(\mathbf{r})$ term, we have included them in the summation over ϕ_i that appears in the Hamiltonian. In the supercell scheme, all these fields have nonzero Fourier components for $\mathbf{q}=\mathbf{G}$ only. The Fourier transform of these potentials are given by the following expressions:

(a) The potential due to the nonhomogeneous positive background (strips of uniform positive charge with width W) is given by

$$\phi_b(\mathbf{G}) = - \left[\frac{e^2}{l}\right] \frac{\nu}{|G_y|l} \left[\frac{\sin(G_y W/2)}{G_y W/2} \right]$$

$$\times e^{-G_y^2 l^2/4}\delta_{G_x,0}(1-\delta_{\mathbf{G},0}) . \tag{8}$$

(b) The confining potential acting on one strip is taken as

$$\phi_c = \begin{cases} 0, & \text{if } |y| < x_0 \\ eV_c\left[\dfrac{|y|-x_0}{\dfrac{A}{2}-x_0}\right], & \text{if } x_0 < |y| < \dfrac{A}{2} \end{cases} \tag{9}$$

so that

$$\phi_c(\mathbf{G}) = V_c l \left[\frac{e^2}{l}\right] \left[\frac{\sin(G_y A/2)}{G_y A/2} \right.$$

$$\left. + \frac{\cos(G_y A/2)-\cos(G_y x_0)}{(G_y A/2)^2(1-2x_0/A)} \right]$$

$$\times e^{-G^2 l^2/4}\delta_{G_x,0} . \tag{10}$$

(c) For the pinning potential, which we take as a Gaussian trap fixed at the center of each *supercell*, we have in real space

$$\phi_p(\mathbf{r}) = V_p \sum_{\mathbf{R}_i} e^{-(\mathbf{r}-\mathbf{R}_i)^2/2l^2} , \tag{11}$$

where $\mathbf{R}_i$ is defined in Eq. 1. Its Fourier transform is

$$\phi_p(\mathbf{G}) = \left[\frac{e^2}{l}\right]\frac{v_p\nu}{2N_c} e^{-G^2 l^2/2} , \tag{12}$$

where $v_p = -eV_p l/e^2$.

III. CALCULATION OF $\langle\rho(\mathbf{G})\rangle$ AND $\langle\mathbf{j}(\mathbf{G})\rangle$ IN THE HFA

To calculate the order parameters $\langle\rho(\mathbf{G})\rangle$, we use the method of Ref. 11. We briefly summarize here the main steps.

We first introduce the one-particle Green's function

$$G(X,X',\tau) = -\langle Tc_X(\tau)c_{X'}^\dagger(0)\rangle , \tag{13}$$

and define its Fourier transform $G(\mathbf{G},\tau)$ by

$$G(\mathbf{G},\tau) = g^{-1}\sum_{X,X'} G(X,X',\tau)$$

$$\times \exp[-iG_x(X+X')/2]\delta_{X',X-G_y l^2} , \tag{14}$$

so that the components $\langle\rho(\mathbf{G})\rangle$ are connected to the Green's function by the relation

$$\langle\rho(\mathbf{G})\rangle = G(\mathbf{G},\tau=0^-) . \tag{15}$$

Using $\hbar\partial/\partial\tau(\ ) = [H-\mu N,(\ )]$ (μ is the chemical potential of the electrons which we measure with respect to the kinetic energy of the first Landau level), we obtain the equation of motion

$$[i\omega_n+\mu/\hbar]G(\mathbf{G},\omega_n)-\sum_{\mathbf{G}'}\frac{1}{\hbar}[U(\mathbf{G}'-\mathbf{G})+\sum_i\phi_i(\mathbf{G}'-\mathbf{G})]\exp[i\mathbf{G}\times\mathbf{G}'l^2/2]G(\mathbf{G}',\omega_n)=\delta_{\mathbf{G},0}\ ,\qquad(16)$$

where ω_n is a fermionic Matsubara frequency. This last equation can be rewritten as

$$[i\omega_n+\mu/\hbar]G(\mathbf{G},\omega_n)-\sum_{\mathbf{G}'}A(\mathbf{G},\mathbf{G}')G(\mathbf{G}',\omega_n)=\delta_{\mathbf{G},0}$$

$$(17)$$

with

$$A(\mathbf{G},\mathbf{G}')=\frac{1}{\hbar}[U(\mathbf{G}-\mathbf{G}')+\sum_i\phi_i(\mathbf{G}-\mathbf{G}')]$$

$$\times\exp[i\mathbf{G}\times\mathbf{G}'l^2/2]\ .\qquad(18)$$

The problem is now reduced to that of finding the eigenvalues and eigenvectors of $A(\mathbf{G},\mathbf{G}')$ that are defined by

$$\sum_{\mathbf{G}'}A(\mathbf{G},\mathbf{G}')V(\mathbf{G}',j)=V(\mathbf{G}',j)\omega_j\ .\qquad(19)$$

We can now perform a Matsubara frequency sum to get, at $T=0$ K,

$$\langle\rho(\mathbf{G})\rangle=\sum_{j=1}^{j_{\max}}V(\mathbf{G},j)[V(\mathbf{G}=0,j)]^*\ ,\qquad(20)$$

where $j_{\max}$ must be determined by the condition that

$$\langle\rho(0)\rangle=\nu\ .\qquad(21)$$

The system of Eqs. (19)–(21) must be solved self-consistently, in an iterative way, until the order parameters $\langle\rho(\mathbf{G})\rangle$ converge to a fixed value. In general, we found that relatively good convergence could be obtained by keeping ≈ 600 values of $\mathbf{G}$ for systems with five or fewer electrons per unit cell.

A problem arises, however, due to the fact that the Hartree-Fock equations of motion may have many different solutions corresponding to local minima in the mean-field energy, which is given by

$$E_{\mathrm{HF}}=\frac{\hbar\omega_c}{2}+\frac{1}{2\nu}\sum_{\mathbf{G}}\left[H(\mathbf{G})(1-\delta_{\mathbf{G},0})-X(\mathbf{G})\right.$$

$$\left.+2\sum_i\phi_i(\mathbf{G})\right]|\langle\rho(\mathbf{G})\rangle|^2\ .\qquad(22)$$

Because the phase space of the order parameters is so large, it is necessary to find a reasonable initial guess for $\langle\rho(\mathbf{G})\rangle$, which is required to start the iteration process. Since we are mainly interested in the domain of filling factor $\nu\le\frac{1}{5}$, we choose, for this initial solution, the classical result[12] corresponding to electrons localized around each lattice site in Gaussian wave packets. In the absence of any confining or pinning potential, the classical density pattern is given approximately by

$$\langle n(\mathbf{r})\rangle=\frac{1}{2\pi l^2}\sum_{i,\alpha}\exp[-(\mathbf{r}-\mathbf{R}_{i,\alpha})^2/2l^2]\ ,\qquad(23)$$

or, in Fourier space,

$$\langle\rho(\mathbf{G})\rangle=\frac{\nu}{N_c}\left[\sum_\alpha e^{-i\mathbf{G}\cdot\mathbf{R}_\alpha}\right]e^{-G^2l^2/4}\ ,\qquad(24)$$

where the summation is over the positions of the electrons in a unit cell. The exact classical positions of the electrons in a unit cell can be obtained, for the general case, by finding a classical potential-energy minimum, as we discuss in the next section. In any case, we find that Eq. (24) is generally a good seed for the iteration process. In some cases, particularly those in which the edge potential is moderately steep, we have found it convenient to start from a weak edge potential, find the solution of the HFA with a classical seed, increment the edge potential, and use the previous solution as a seed for the new problem. In this way, we can work our way up to moderate and strong confinement potentials.

We iterate the Hartree-Fock equations with the initial solution until we obtain convergence. As we show in the next section, we can check the stability of any solution by calculating the collective mode spectrum corresponding to small oscillations around the mean-field solution.

We end this section by a discussion of the ground-state current density. In the first Landau level, the instantaneous current density is completely transverse. As discussed in Ref. 13, this is merely a reflection of the fact that the kinetic energy has been quenched, and perturbations can cause particles to move only by means of virtual transitions to higher Landau levels. We can, however, define another current operator which does not include the fast cyclotron motion, but instead retains only the slow $\mathbf{E}\times\mathbf{B}$ drift motion of the particles in the magnetic field. To do this, following Ref. 13, we write the equation of motion for the density operator ρ in the lowest Landau level. We find

$$\frac{\partial}{\partial t}\langle\rho(\mathbf{G})\rangle=\frac{2}{\hbar}\sum_{\mathbf{G}'}W(\mathbf{G}')\sin(\mathbf{G}'\times\mathbf{G}l^2/2)\langle\rho(\mathbf{G}'+\mathbf{G})\rangle\ ,$$

$$(25)$$

where

$$W(\mathbf{G})=U(\mathbf{G})+\sum_i\phi_i(\mathbf{G})\ .\qquad(26)$$

For a slowly varying field, i.e., for $W(\mathbf{G})/(e^2/l)\ll 1$ when $Gl>1$, we can write

$$\sin(\mathbf{G}'\times\mathbf{G}l^2/2)\approx\mathbf{G}\cdot(\hat{z}\times\mathbf{G}')l^2/2\ .\qquad(27)$$

Comparing then Eq. (25) with the continuity equation

$$-ege^{-G^2l^2/4}\frac{\partial}{\partial t}\langle\rho(\mathbf{G})\rangle=-i\mathbf{G}\cdot\langle\mathbf{j}(\mathbf{G})\rangle\ ,\qquad(28)$$

we finally get, for the current operator in the lowest Landau level,

$$\langle\mathbf{j}(\mathbf{G})\rangle=\frac{-eigl^2}{\hbar}e^{-G^2l^2/4}$$

$$\times\sum_{\mathbf{G}'}W(\mathbf{G}')(\hat{z}\times\mathbf{G}')\langle\rho(\mathbf{G}'+\mathbf{G})\rangle\ .\qquad(29)$$

In real space, this expression becomes (always in the slowly varying field approximation),

$$\langle \mathbf{j}(\mathbf{r}) \rangle = \frac{e^2 l^2}{\hbar} [\nabla W(\mathbf{r}) \times \hat{z}] \langle n(\mathbf{r}) \rangle \; , \qquad (30)$$

using Eq. (5). We note that Eq. (30) is consistent with some recent expressions derived via density-functional theory that relate the current to the electron density in a magnetic field.[14]

IV. COLLECTIVE MODE SPECTRUM IN THE GRPA

The collective excitations of the crystal are poles of the density-density response function,[11] which is defined by

$$\chi_{\mathbf{G},\mathbf{G}'}(\mathbf{k},\tau) = -g \langle T\tilde{\rho}(\mathbf{k}+\mathbf{G},\tau)\tilde{\rho}(-\mathbf{k}-\mathbf{G}',0) \rangle \; , \qquad (31)$$

where $\mathbf{k}$ is a vector in the first Brillouin zone of the crystal and $\tilde{\rho}=\rho-\langle\rho\rangle$. As for the calculation of the one-particle Green's function, we use the Hamiltonian of Eq. (6) to derive the equation of motion of this correlation function in the Hartree-Fock approximation (i.e., one loop approximation χ^0). Using the commutation relation of the density operators in the Hilbert space of the lowest Landau level,

$$[\rho(\mathbf{q}),\rho(\mathbf{q}')] = 2ig^{-1}\rho(\mathbf{q}+\mathbf{q}')\sin(\mathbf{q}\times\mathbf{q}'l^2/2) \; , \qquad (32)$$

$$\sum_{\mathbf{G}''} [i\Omega_n \delta_{\mathbf{G},\mathbf{G}''} - C_{\mathbf{G},\mathbf{G}''}(\mathbf{k})]\chi^0_{\mathbf{G}'',\mathbf{G}'}(\mathbf{k},\Omega_n) = D_{\mathbf{G},\mathbf{G}'}(\mathbf{k}) \; , \qquad (33)$$

where

$$C_{\mathbf{G},\mathbf{G}'}(\mathbf{k}) = \left[\frac{2i}{\hbar}\right]\left[U(\mathbf{G}-\mathbf{G}')+\sum_i \phi_i(\mathbf{G}-\mathbf{G}')\right] \times \sin[(\mathbf{k}+\mathbf{G})\times(\mathbf{k}+\mathbf{G}')l^2/2] \; , \qquad (34)$$

and

$$D_{\mathbf{G},\mathbf{G}'}(\mathbf{k}) = -2i\langle\rho(\mathbf{G}-\mathbf{G}')\rangle \times \sin[(\mathbf{k}+\mathbf{G})\times(\mathbf{k}+\mathbf{G}')l^2/2] \; . \qquad (35)$$

χ^0 does not include the correlations that give rise to the phonons of the electron crystal. In order to include these correlations, we calculate the density response function in the GRPA. This calculation is given in detail in Ref. 11. The final result for the response function is

$$\sum_{\mathbf{G}''}\left[i\Omega_n\delta_{\mathbf{G},\mathbf{G}''} - C_{\mathbf{G},\mathbf{G}''}(\mathbf{k}) - \frac{1}{\hbar}D_{\mathbf{G},\mathbf{G}''}(\mathbf{k})[H(\mathbf{k}+\mathbf{G}'')-X(\mathbf{k}+\mathbf{G}'')]\right]\chi_{\mathbf{G}'',\mathbf{G}'}(\mathbf{k},\Omega_n) = D_{\mathbf{G},\mathbf{G}'}(\mathbf{k}) \; . \qquad (36)$$

As is seen from Eq. (36), the response function is completely determined once the order parameters $\langle\rho(\mathbf{G})\rangle$ are known. The dispersion relation of the collective modes are found by tracking the poles of χ for several values of the wave vector $\mathbf{k}$.

It is of interest to compare the above quantum results (HFA and GRPA) to those of the classical crystal in which the electrons are viewed as rigid blocks oscillating around their equilibrium position. Their instantaneous positions are given [see Eq. (1)] by the vectors

$$\mathbf{r}_{i,\alpha}(t) = \mathbf{R}_i + \mathbf{r}_\alpha + \mathbf{u}_{i,\alpha}(t) \; , \qquad (37)$$

where $\mathbf{u}_{i,\alpha}(t)$ represents the displacement of the electron α in the unit cell i. We define the Fourier transform of this displacement as

$$\mathbf{u}_\alpha(\mathbf{k},t) = \sum_i \mathbf{u}_\alpha(t)e^{-i\mathbf{k}\cdot\mathbf{R}_i} \; . \qquad (38)$$

The density pattern of the classical crystal is thus given by

$$n(\mathbf{r},t) = \sum_{i,\alpha} h[\mathbf{r}-\mathbf{r}_{i,\alpha}(t)] \; , \qquad (39)$$

where the rigid envelope $h(\mathbf{r})$ of the electron is given by [see Eq. (23)]

$$h(r) = \frac{1}{2\pi l^2}\exp[-r^2l^2/2] \; . \qquad (40)$$

To find the dispersion relations of the collective modes, one needs to write a linearized equation of motion for the displacement $\mathbf{u}_\alpha(\mathbf{k},\omega)$. Using Newton's law, this is given by

$$-m\omega^2\mathbf{u}_\alpha(\mathbf{k},\omega) = \sum_n \mathbf{F}_\alpha^{(n)}(\mathbf{k},\omega) \; , \qquad (41)$$

where the $\mathbf{F}_\alpha^{(n)}$ are the forces acting on the electron α including the Lorentz force and the force due to all the other electrons. After a straightforward calculation, we find that

$$\sum_\beta\left[\left[\mathcal{J}\omega^2 - \sum_i \chi_\alpha^{(i)} - \omega\omega_c\sigma_y\right]\delta_{\alpha,\beta} - \mathcal{D}_{\alpha,\beta}\right]\cdot\mathbf{u}_\beta(\mathbf{k},\omega) = 0 \; , \qquad (42)$$

where $\mathcal{J}$ is the 2×2 unit matrix, σ_y is a Pauli matrix, $\mathcal{D}_{\alpha,\beta}$ is the dynamical matrix of the electron lattice, which is given by

$$\mathcal{D}_{\alpha,\beta}(\mathbf{k}) = \frac{2\pi e^2 N}{mN_c}\sum_{\mathbf{G}}\left[\frac{(\mathbf{k}+\mathbf{G})(\mathbf{k}+\mathbf{G})h^2(\mathbf{k}+\mathbf{G})}{|\mathbf{k}+\mathbf{G}|}\right.$$
$$\times e^{i(\mathbf{k}+\mathbf{G})\cdot(\mathbf{r}_\alpha-\mathbf{r}_\beta)}$$
$$\left.- \frac{\mathbf{G}\mathbf{G}h^2(\mathbf{G})}{|\mathbf{G}|}\delta_{\alpha,\beta}\sum_\delta e^{i\mathbf{G}\cdot(\mathbf{r}_\delta-\mathbf{r}_\alpha)}\right] \; , \qquad (43)$$

and

$$\chi_\alpha^{(i)} = \frac{e}{mS}\sum_{\mathbf{G}}\mathbf{G}\mathbf{G}h(\mathbf{G})\phi_i(\mathbf{G})e^{i\mathbf{G}\cdot\mathbf{r}_\alpha} \; , \qquad (44)$$

is a 2×2 matrix representing the influence of the external

forces (positive background, confinement, pinning) with $\phi_i(\mathbf{G})$ defined in Eqs. (8), (10), and (12).

Diagonalization of Eq. (42) gives all the collective modes of the electron lattice in the presence of the external forces. In particular, for a lattice of one electron per unit cell, there will be one magnetophonon and one magnetoplasmon mode. As was emphasized in Ref. 11, the magnetoplasmon excitation is an inter-Landau-level excitation and thus is not present in the quantum density response function calculated above using only one Landau level. Instead, χ corresponds to an approximation of Eq. (42) in which the various resonant frequencies of the external forces are much less than the cyclotron frequency ω_c. A completely equivalent statement is to write Eq. (42) without the inertial term $\mathcal{J}w^2$. The problem is then reduced to that of finding the eigenvalues of a $2N_c \times 2N_c$ matrix. The modes found in this way correspond to intra-Landau-level excitations only.

Finally, we note that the condition for the equilibrium of the different forces on an electron β is expressed, classically, as

$$\sum_{\mathbf{G}} e^{i\mathbf{G}\cdot\mathbf{r}_\beta}\mathbf{G}\left[\left[\frac{e^2}{l}\right]\frac{v}{N_c|\mathbf{G}|}h^2(\mathbf{G})\sum_\alpha e^{-i\mathbf{G}\cdot\mathbf{r}_\alpha}\right.$$
$$\left. + h^{1/2}(\mathbf{G})\sum_i \phi_i(\mathbf{G})\right] = 0 \ . \quad (45)$$

The classical equilibrium position of the electrons in the presence of the external fields can be found by searching for solutions of Eq. (45) as a function of the positions $\mathbf{r}_\beta$. The resulting electron density may then be used as an initial guess to start the iteration process for the Hartree-Fock self-consistent $\langle\rho(\mathbf{G})\rangle$.

V. NUMERICAL RESULTS

We begin with a discussion of the results of the HFA for the density profiles of this system. Typical contour plots for the density are presented in Fig. 1 for several values of the edge potential strength V_c (in units of $1/l$). In these figures, we have taken $v=\frac{1}{7}$ and $N_c=5$. In Fig. 1(a), the case of $V_c=0$ is illustrated, for which the confinement potential is due only to the finite neutralizing

background charge. Each electron is spread out in a wave packet of size l, since we are considering only ground states in the lowest Landau level; this finite spread of the individual electronic wave functions is thus a consequence of the zero-point (quantum) motion of the electrons, and we will see that this plays a crucial role in the edge melting phenomenon. We note that the triangular lattice in the bulk of the system is essentially undisturbed, with only a small *inward* relaxation of the rows closest to the crystal edge. The inward relaxation is purely an electrostatic effect, and we have confirmed in a classical electron system that this is expected to occur, using Eq. (45).

As the parameter V_c is increased in magnitude, one can see that the initial effect is to compress the rows of electrons nearest the edge together, as is clear in Figs. 1(b) and 1(c) ($V_c=1.0$ and 2.0, respectively). This is once again a classical effect, and it should be noted that this type of reconfiguration is unique to the Coulomb interaction. For short-range interactions, one would expect that pushing on the crystal at its edge would cause a small increase in the *bulk* density of electrons. However, since we require a neutralizing positively charged background in the Coulomb system, a bulk increase in density becomes prohibitively large in energy, since this would force the system to maintain a charge imbalance over macroscopic distances. Thus, the main response of the electron gas to the confining potential is localized to the edge of the sample. This means that the local electron density at the edge is *higher* than in the bulk. We should note that such a situation is experimentally attainable if the edge potential is turned on at low temperatures. In this case, there is a high thermal barrier for electrons to diffuse back to the charged donors, which play the role of the neutralizing background. One thus has a fixed neutralizing charge, and our system for which electron charge is conserved as a function of the confinement potential is appropriate. It is important to note that at higher temperatures, the electrons could recombine with charged donors, leading to a degrading of the electron density at the edge.

Figures 1(c) and 1(d) are actually two separate configurations of electrons at $V_c=2.0$; both are solutions to the HFA. It is clear that the difference between the
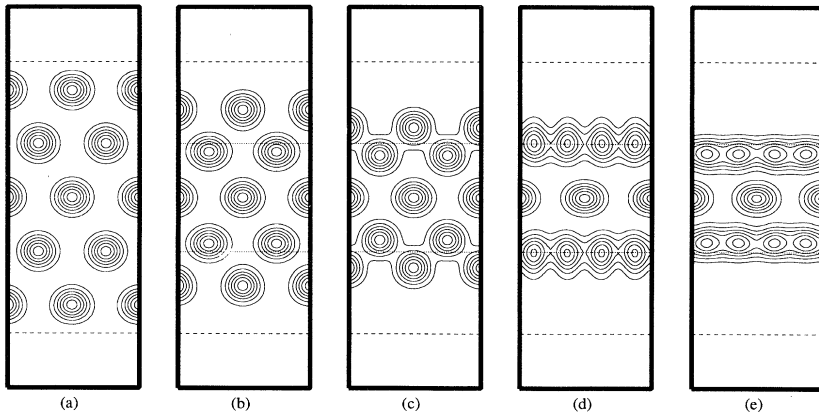

FIG. 1. Hartree-Fock density patterns for different values of the confining potential V_c showing edge reconstruction and edge melting. (a) $V_c=0.0$; (b) $V_c=1.0$; (c), (d) $V_c=2.0$; (e) $V_c=10.0$. (Parameters are $N_c=5$, $A=7\sqrt{3}/2$, $W=5\sqrt{3}/2$, $x_0=\sqrt{3}/2$, $\xi=1$, $v=1/7$. V_c is in units of l^{-1}.)

two configurations is that the two rows of electrons closest to the edge have merged in the second configuration. We find that these two types of solutions can both be stabilized in a range $\sim 1.5 \leq V_c \leq \sim 2.5$, with solutions of the type illustrated in 1(c) lower in energy at the lower V_c end of the range, and solutions such as 1(d) lower at the higher end of the range. This means that at a critical value of V_c, the edge configuration will go through a sudden change. *This is a reconstruction of the edge electrons,* and clearly in this example it is a first-order transition.[15] We will see below that such a transition has a clear signal in the collective mode response of the system.

At and above the potentials for which one reaches configurations such as that illustrated in Fig. 1(d), zero-point motion effects begin to become important: the individual electron orbits are no longer well defined, and begin to merge. At stronger confinement potentials [Fig. 1(e), $V_c = 10.0$], the transverse density oscillations with the rows of electrons from which the high-density edge is formed are nearly gone; the configuration at the edge looks more fluidlike than crystallike. This is a *melting* transition for the edge electrons, and we will see below that it has a definite consequence: the electrons in the melted edge are not pinned (at least within the HFA) by bulk disorder, as they are for a solid edge. We will see below that when one computes the response function in the presence of bulk pinning centers, all the collective modes will be gapped for cases 1(a)–1(d); however, case 1(e) turns out to have a *gapless* mode, suggesting that it can support a current. This means that the edge melting transition is a kind of metal-insulator transition, and could be detected in transport experiments, as discussed below.

To support this interpretation, we have computed the density of states for the system within the HFA. This is defined for an interacting system as

$$D(E) = -\frac{1}{S} \sum_X G(X,X;E) \ ,$$

where S is the system area. It is not difficult to show that this may be rewritten as

$$D(E) = -\frac{g}{S} \text{Im} G(\mathbf{G}=0, i\omega_n = E)$$

$$= -\frac{1}{2\pi l^2} \text{Im} \sum_j \frac{|V(\mathbf{G}=0,j)|^2}{E - \omega_j + i\delta} \ .$$

Figure 2 illustrates $D(E)$ for several values of V_c. In Fig. 2(a), we display the case $V_c = 0$ [corresponding to Fig. 1(a)], along with the position of the chemical potential μ. One can see that μ falls in a large gap region of $D(E)$. This implies that charged excitations require a finite energy, so that at low temperatures, the bulk WC is an insulator. However, as V_c is raised, some of the single-particle states break off from the high-energy peak in $D(E)$ [Fig. 2(b), corresponding to Fig. 1(d)], and begin to move to lower energies, although the chemical potential still lies in a gap. (We note that the small but nonvanishing value of $D(E)$ at the chemical potential is due to using a finite value of δ; there are no states with non-vanishing weight

in the gap region.) Finally, at the melting transition [Fig. 2(c), corresponding to Fig. 1(e)], the gap in which the chemical potential lies has completely closed up. Within mean-field theory, the interpretation of this situation is that one can generate charged excitations with
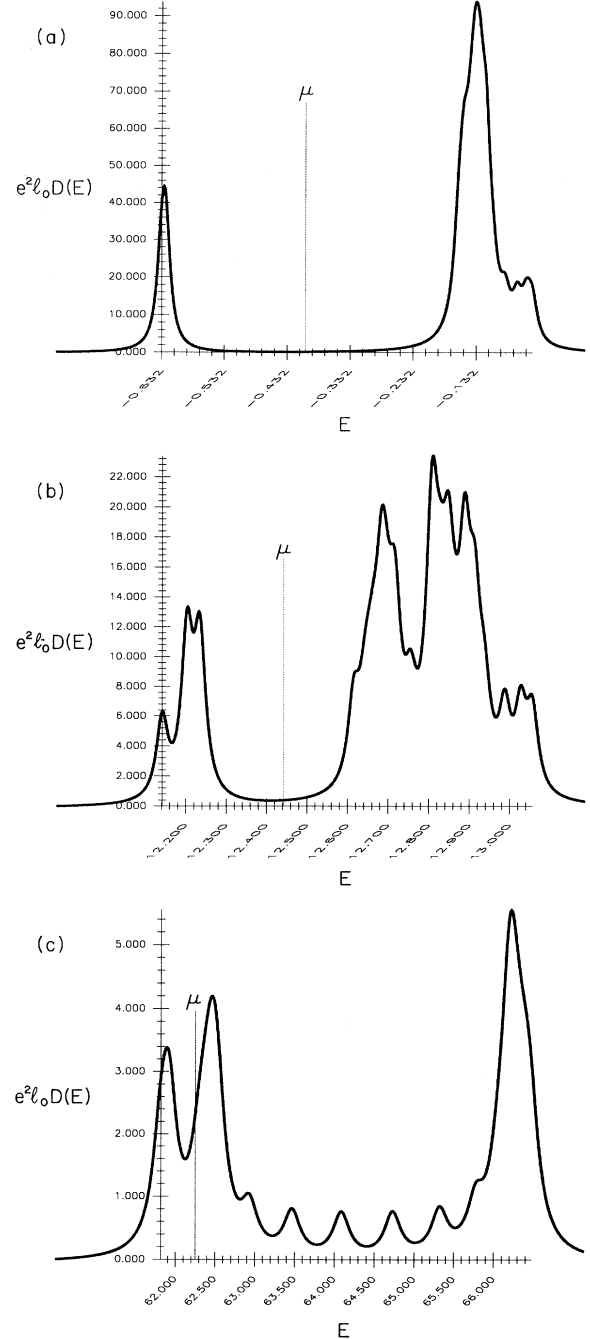

FIG. 2. Density of states in the HFA (in arbitrary units) for different values of the confining potential (in units of l^{-1}). (a) $V_c = 0$ corresponding to Fig. 1(a); (b) $V_c = 2.0$ corresponding to Fig. 1(d); and (c) $V_c = 10.0$ corresponding to melted edge. The vertical line represents the position of the chemical potential at $T = 0$ K. Note that the density of states does vanish at the chemical potential in (b). The finite weight in this figure is a numerical artifact.

infinitesimal energy cost—allowing for a finite (metallic) response to a weak electric field. However, as discussed in the introduction, and as we will discuss further below, it is unclear whether this metallic response actually survives at zero temperature when one goes beyond mean-field theory.

To understand how the edge melting transition occurs in this system, consider the effect of a confinement potential $\phi(y)$ at the edge of a classical WC in a strong magnetic field. We can associate a local drift velocity $\mathbf{v_d} = c\nabla\phi(y)\times\mathbf{B}/eB^2$ with the bare confinement potential ϕ so that a WC spread out over the region in which the confinement potential varies faster than linearly will tend to shear. The system overcomes this by compressing in the $\hat{\mathbf{y}}$ direction, so that the total (self-consistent) electric field at any lattice point on the edge vanishes. In the quantum-mechanical case, however, this compression has a nontrivial effect: any attempt to compress the electron density perpendicular to the edge will necessarily lead to a spreading of the density parallel to the edge. This is most easily seen within mean-field theory. Compression of the charge density near the edge may be accomplished by building the wave function out of single-particle states that fall off more quickly in the $\hat{\mathbf{y}}$ direction than do the circular Gaussian orbitals out of which one may build a WC state in an unbounded WC. However, any compression of a single-particle state in the lowest Landau level in a given direction necessarily leads to spreading of the wavefunction in the orthogonal direction.[16] This is purely a result of zero-point motion of electrons in a strong magnetic field, and may be expressed as an uncertainty relation among guiding center coordinates[16,17] of the electrons $\Delta X \Delta Y \simeq l^2$. Alternatively, one may consider how a WC is built up out of single-particle wave functions of the form

$$\psi_Y(x,y) = \left[\frac{1}{\pi l^2 L^2}\right]^{1/4} \exp[iYx/l^2 - (y-Y)/2l^2] \ .$$

To create states with transverse density oscillations (density oscillations parallel to the edge) of wave vector k_y, one must consider linear combinations of the states Y and $Y+k_y l^2$. However, near the edge, states at large values of $Y+k_y l^2$ will have large energies, so that forming such linear combinations becomes unfavorable. In this way, transverse density oscillations are suppressed near the edge.

Since the edge electrons are liquidlike, and are confined to a region in which there is a potential gradient, it seems reasonable to assume that the edge electrons have a non-vanishing current density. This view is further supported by the fact that one finds a linear mode in the collective excitation spectrum, precisely as in the case of the QHE edge states, which are known to carry current. This turns out to be the case; however, there is a crucial difference between a melted WC edge and the QHE edge: the former is not chiral. In practice, this means that a melted edge in the WC carries no net current, even while there is a nonvanishing current density. To demonstrate this, we have explicitly computed the current density $\langle \mathbf{j}(\mathbf{r}) \rangle$ using Eqs. (29) and (30). Contour plots of j_x are
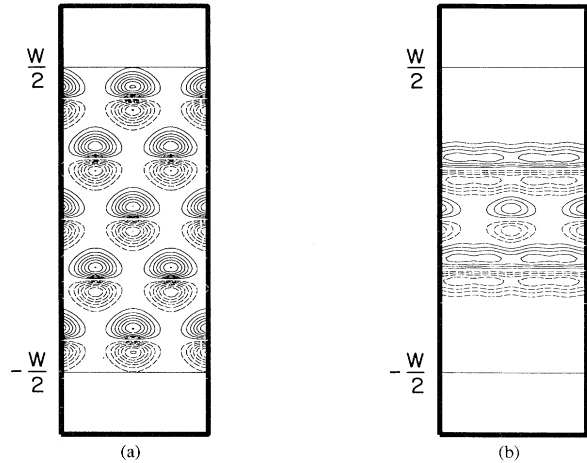

FIG. 3. Ground-state current density $\langle j_x(\mathbf{r}) \rangle$ in the HFA corresponding to (a) Fig. 1(a) (normal edge) and (b) Fig. 1(e) (melted edge). Positive values of $\langle j_x \rangle$ are denoted by solid lines and negative values by dashed lines.

illustrated in Fig. 3. Positive values of $\langle j_x \rangle$ are denoted by solid lines, and negative values by dashed lines in these figures. Figure 3(a) illustrates the case corresponding to the density profiles of Fig. 1(a); one can see that each electron is essentially executing a closed orbit, so that no net current flows through the system. Figure 3(b) is the current density for the same system parameters as in Fig. 1(e); here, we find continuous current flows along the melted edge, but that the current on the inner side of a melted edge runs in the opposite direction of that on the outer side. A numerical integration of the total current carried by the melted edge in the $\hat{\mathbf{x}}$ direction turns out to vanish identically, within the numerical accuracy of our calculation. Indeed, it may be shown on general grounds that so long as one may draw a line through the melted edge between two points where the gradient of the electron density vanishes, the total current through the line must vanish, so long as the ground state of the system lies completely in the lowest Landau level.[14]

Finally, it is worth noting that for values of V_c just above the critical one at which the edge melts, it is rather clear from Figs. 1 and 3 that the resulting system is quasi-one-dimensional, in that there are single-particle (Hartree-Fock) states with currents running in opposite directions, some of which will be physically close to one another on the scale of a magnetic length. It is interesting to consider this as an isolated system, including the bulk electrons only through a periodic potential to which the edge electrons are subject. A model of this sort was analyzed previously within mean-field theory for potentials varying more slowly than those considered here.[7]

In a one-dimensional model, it becomes possible to go beyond mean-field theory, and consider effects of quantum fluctuations on the interacting system. In the absence of a periodic potential, fluctuations are known to cause a breakdown of mean-field theory, leading to a system known as a Luttinger liquid. This system, a Luttinger liquid in a periodic potential, was analyzed in some

detail recently by Kolomeisky.[9] It was found that as a function of the electron-electron coupling and the product of the linear electron density with the external potential period, there will be a phase boundary separating *pinned* states from *conducting* states. It is interesting to note that one may actually investigate a large range of the phase diagram of this system using the edge melting phenomenon: by increasing the edge potential, one increases the linear (edge) electron density, and by varying the magnetic field, one may change the scattering amplitude between left-moving and right-moving states, which effectively changes the interelectron coupling.

Thus, although the HFA approximation predicts that the melted edge should be conducting, so that one obtains metallic behavior right at the melting transition, we find from the considerations of Ref. 9 that the melted edge could be pinned at zero temperature, depending where precisely the system ends up on the phase diagram. However, even if this is the case, it is still possible to detect the edge melting in a *finite* temperature transport experiment: for the pinned Luttinger liquid, the conductance vanishes as a power law T^p at low temperatures, whereas for a conventional WC the conductance is expected to vanish exponentially. We note that recent work[8] on the effects of impurities on transport in the Luttinger liquid leads to a similar prediction for finite temperature transport. Thus, the phenomenon of edge melting allows for an experimental realization of the Luttinger liquid in a periodic (and, inevitably, a disorder) potential, which should have some unique and interesting transport properties.

We now turn to our results for the collective edge modes of the WC. In the GRPA, the collective modes corresponding to intra-Landau-level excitations are given by the poles of the density-density response function $\chi_{G,G}(\mathbf{k},\omega)$. As we see from the equation of motion of χ [Eq. (36)], this function is completely determined once the order parameters $\langle \rho(\mathbf{G}) \rangle$ are known for a given value of the confining potential. In Fig. 4, we have plotted the dispersion relation of the first five modes obtained from the GRPA for the density profile corresponding to Fig.
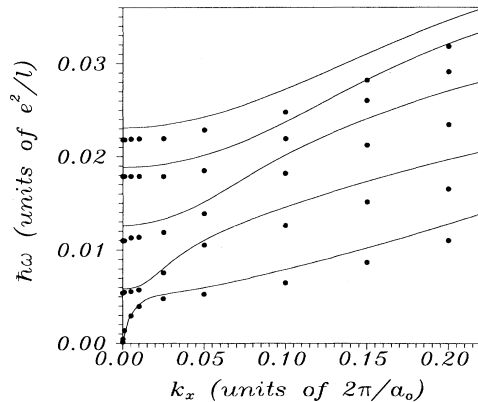
1(a); i.e., for no confining potential. These five modes are in direct correspondence with the five classical modes of vibration of a system with five electrons per unit cell. There should be, of course, ten modes, for a 2D system, but we have made the approximation of keeping only the first Landau level in our calculation of χ, so that all the inter-Landau-level modes are lost. As we mentioned above, we can calculate the dispersion relation of these five modes for a classical harmonic lattice by first calculating the equilibrium positions of the five electrons using Eq. (45), and then solving Eq. (42) without the inertial term. This harmonic result is represented by the full lines in Fig. 4. The difference between the GRPA and harmonic results are due to anharmonic and quantum corrections (such as the deformation of the wave function of the vibrating electrons) not included in the simple calculation leading to Eq. (42). While there are some differences, one can see that the qualitative behavior of the various modes agree fairly well, especially in the long-wavelength limit. (We have exploited this agreement between the quantum and classical calculations to understand the low-energy spectrum of the WC at a soft edge in a previous publication.[6]) In the remainder of this paper, we shall concentrate on the lowest-energy mode only.

In the absence of a confining potential, we see from Fig. 4 that the lowest mode is gapless, and for $k_y = 0$ disperses as $k_x^{1/2}$. This result contrasts with the usual $k^{3/2}$ dispersion of the infinite crystal.[18] The hardening of this low-energy mode is simply a result of the restoring force on the electrons in one direction due to the inhomogeneous neutralizing background. This can easily be seen by assuming a uniform motion, $\mathbf{u}_\beta(\mathbf{k}) \rightarrow \mathbf{u}(\mathbf{k})$, of all the electrons in the unit cell in the lowest-energy mode in the small $\mathbf{k}$ limit. The problem of solving Eq. (42) is then reduced to that of diagonalizing a 2×2 matrix and expanding in powers of k (see Ref. 19). In the presence of a pinning potential, we would expect from similar considerations that this lowest-energy mode would exhibit a gap
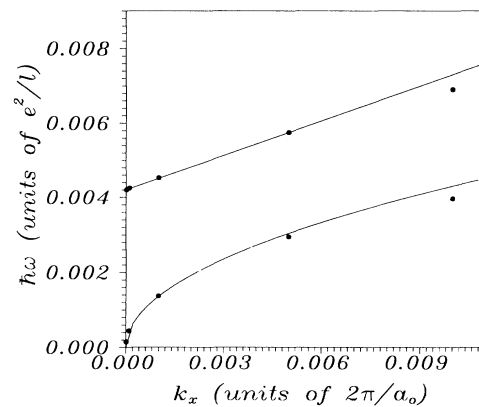

FIG. 4. A comparison of the dispersion relation of the five lowest collective modes calculated in the GRPA ($\bullet$) and in the classical harmonic approximation (full lines) for the density pattern of Fig. 1(a). ($k_y = 0.0$.)

FIG. 5. Dispersion relation of the lowest collective mode for normal edge [pattern of Fig. 1(a)]. The lower (upper) set of points ($\bullet$) is for $\omega(\mathbf{k})$ in the absence (presence) of pinning. The full lines are a fit with the expected dispersion relation at small $\mathbf{k}$ (see text); i.e., square root in the absence of pinning and linear dispersion in the presence of pinning ($v_p = -0.25$, $k_y = 0$).
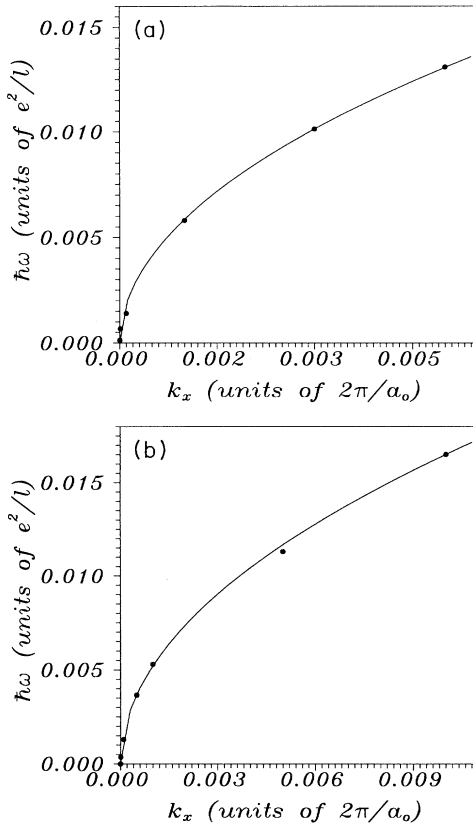
FIG. 6. Dispersion relation of the lowest collective mode for the melted edge [density pattern of Fig. 1(e)]: (a) without pinning and (b) with pinning. The full lines are a fit with a square root dispersion relation $(v_p = -0.25, k_y = 0)$.

proportional to the pinning force and would disperse linearly with k_x (at $k_y = 0$). To see that this is indeed the case, we have plotted in Fig. 5 the dispersion relation of the lowest-energy mode of Fig. 4 in the presence of a pinning potential consisting of a single Gaussian trap at the center of each supercell (see Sec. III). As expected, the WC becomes an insulator in the presence of disorder, since it takes a finite electric field to unpin the crystal and produce a current. We have verified that a similar behavior of the low-energy mode occurs for the other density patterns represented in Figs. 1(b)–1(d).

The situation changes radically when the edge is melted [density pattern of Fig. 1(e)]. In that case, the dispersion relation of the lowest collective mode is represented in Figs. 6(a) and 6(b). We see that there is also a gapless mode in the absence of pinning for the melted edge. However, this mode remains gapless when the pinning potential is added, showing that the density wave of the melted edge is not pinned by disorder, in contrast to the normal edge. We believe that the presence of such a gapless mode may be a defining property for the edge melting transition.

Strictly speaking, our pinning potential is periodic, so we are not dealing with true disorder in this model. However, this approximation for the response function in the presence of bulk pinning is analogous to the uniform pinning approximations used in simple phenomenological treatments of charge-density waves.[20] Thus, our periodic pinning potential should be understood as a washboard potential. Within our formalism, a more sophisticated microscopic treatment of disorder seems to be prohibitively difficult.

The dispersion relation derived above corresponds to a superlattice of WC strips. Our aim, however, is to consider the single-strip case. As we already pointed out, this would mean taking the limit where $A \to \infty$. Because the number of reciprocal-lattice vectors increases very rapidly with A/W, it is numerically impossible to treat realistic values of A/W. In the present work, we have set $A = 7\sqrt{3}/2$, $A/W = \frac{7}{5}$, and $x_0 = \sqrt{3}/2$. We have also examined systems with unit cells twice as large, and found no qualitative change in our results. Indeed, the physical explanation of the edge melting given above is quite general, so that melting should occur for large systems as well. For finite A/W values, we expect the dispersion relation to show the single-strip behavior (a low-energy mode dispersing as $k\sqrt{|\ln(k)|}$ in agreement with the result for one-dimensional systems[21]) for wave vectors in the range $1/A \ll k_x \ll 1/W$. For the above values of A and W, this range is quite small. However, our aim in this paper was to demonstrate the metal-insulator character of the edge melting transition. It should thus be kept in mind that if the superlattice has a gapless mode, then so must also the single strip. This is due to the fact that, quite generally, screening effects in a superlattice tend to *lift* gapless collective modes over what one expects in an isolated system.[22] Thus, a gapless mode in the superlattice case necessarily implies the presence of one for the single strip geometry.

VI. CONCLUSION

We have investigated the edge electronic structure for electrons in a Wigner crystal state, and found that with increasing confinement potential strengths, the edge electrons undergo a reconstruction followed by a melting transition. In contrast to the crystal state, the state in which an edge has melted has a gapless collective mode, even in the presence of bulk pinning centers, and can thus carry a current. The edge melting transition can then be thought of as an insulator-to-metal transition, within mean-field theory.

Correlations beyond mean-field theory may change this conclusion about the transport properties of the melted edge, depending on the degree of disorder and the strength of the coupling to the bulk WC. However, we find that an appropriate model predicts an unusual power-law temperature dependence for the conductivity of this system, even if the zero-temperature state of the melted edge is pinned. It should also be possible to probe both the pinned and conducting states by varying the magnetic field and/or the confining potential strength. In any case, the edge melting transition of this system is a unique manifestation of quantum effects in the magnetically induced WC, and has many interesting experimental consequences.

[1]E. P. Wigner, Phys. Rev. **46**, 1002 (1934).

[2]C. C. Grimes and G. Adams, Phys. Rev. Lett. **42**, 795 (1979).

[3]For the observation of the WC in zero magnetic field in the Si inversion layer, see, for example, S. V. Kravchenko, V. M. Pudalov, J. Campbell, and M. D'Iorio, Pis'ma Zh. Eksp. Teor. Fiz. **54**, 528 (1991) [JETP Lett. **54**, 532 (1991)], and references cited therein.

[4]V. J. Goldman, M. Santos, M. Shayegan, and J. E. Cunningham, Phys. Rev. Lett. **65**, 2189 (1990); H. W. Jiang, R. L. Willett, H. L. Stormer, D. C. Tsui, L. N. Pfeiffer, and K. W. West, *ibid.* **65**, 633 (1990); Y. P. Li, T. Sajoto, L. W. Engel, D. C. Tsui, and M. Shayegan, *ibid.* **67**, 1630 (1991); E. Andrei *et al.*, *ibid.* **60**, 2765 (1988); F. I. B. Williams *et al.*, *ibid.* **66**, 3285 (1991); M. D'Iorio, V. M. Pudalov, and S. G. Semenchinsky, Phys. Lett. A **150**, 422 (1990).

[5]See, for example, M. Stone, Ann. Phys. (N.Y.) **207**, 38 (1991) and work cited therein.

[6]H. A. Fertig and R. Côté, Phys. Rev. B **48**, 2391 (1993).

[7]H. A. Fertig and S. Das Sarma, Surf. Sci. **263**, 60 (1992); Phys. Rev. B **47**, 10 484 (1993).

[8]C. Kane and M. P. A. Fisher, Phys. Rev. Lett. **68**, 1220 (1992).

[9]E. B. Kolomeisky, Phys. Rev. B **47**, 6193 (1993).

[10]H. A. Fertig, R. Côté, A. H. MacDonald, and S. Das Sarma, Phys. Rev. Lett. **69**, 816 (1992).

[11]R. Côté and A. H. MacDonald, Phys. Rev. Lett. **65**, 2662 (1990); Phys. Rev. B **44**, 8759 (1991).

[12]K. Maki and X. Zotos, Phys. Rev. B **28**, 4349 (1983).

[13]S. M. Girvin, A. H. MacDonald, and P. M. Platzman, Phys. Rev. B **33**, 2481 (1986).

[14]G. Vignale and P. Skudkarski, Phys. Rev. B **46**, 10 232 (1992).

[15]We have found, however, that for other situations (e.g., higher fields or large unit cells) the transition may often be smooth, so that in some cases one would expect a second-order transition. However, for large enough systems, where several rows of electrons may need to merge as the edge potential is increased, it is likely that such transitions will in general be *first* order, since the electrons in the high density row will need to rearrange in order to accommodate a new row of electrons.

[16]For a review of the decomposition into cyclotron and guiding center coordinates, see R. Kubo *et al.*, in *Solid State Physics: Advances in Research and Applications*, edited by F. Seitz and D. Turnbull (Academic, New York, 1965), Vol. 17.

[17]The guiding center coordinates of an electron locate the center of its cyclotron orbit in a strong magnetic field. They should not be confused with the real electron coordinates.

[18]L. Bonsall and A. A. Maradudin, Phys. Rev. B **15**, 1959 (1977).

[19]R. Côté and A. H. MacDonald, Surf. Sci. **263**, 187 (1992).

[20]P. B. Littlewood, Phys. Rev. B **33**, 6694 (1986); D. S. Fischer, *ibid.* **31**, 1396 (1985); P. A. Lee and T. M. Rice, *ibid.* **19**, 3970 (1979).

[21]Q. P. Li and S. Das Sarma, Phys. Rev. B **43**, 11 768 (1991).

[22]S. Das Sarma and J. J. Quinn, Phys. Rev. B **25**, 7603 (1982).